
H2RBox-v2: Boosting HBox-supervised Oriented Object Detection via Symmetric Learning

Yi Yu^{1*}, Xue Yang^{2*}, Qingyun Li³, Yue Zhou², Gefan Zhang^{2,4}, Feipeng Da^{1†}, Junchi Yan^{2†}

¹Southeast University ²Shanghai Jiao Tong University

³Harbin Institute of Technology ⁴COWAROBOT Co. Ltd.

yuyi@seu.edu.cn, yangxue-2019-sjtu@sjtu.edu.cn

PyTorch Code: <https://github.com/open-mmlab/mrotate>

Jittor Code: <https://github.com/Jittor/JDet>

Abstract

With the increasing demand for oriented object detection e.g. in autonomous driving and remote sensing, the oriented annotation has become a labor-intensive work. To make full use of existing horizontally annotated datasets and reduce the annotation cost, a weakly-supervised detector H2RBox for learning the rotated box (RBox) from the horizontal box (HBox) has been proposed and received great attention. This paper presents a new version, H2RBox-v2, to further bridge the gap between HBox-supervised and RBox-supervised oriented object detection. While exploiting axisymmetry via flipping and rotating consistencies is available through our theoretical analysis, H2RBox-v2, using a weakly-supervised branch similar to H2RBox, is embedded with a novel self-supervised branch that learns orientations from the symmetry inherent in the image of objects. Complemented by modules to cope with peripheral issues, e.g. angular periodicity, a stable and effective solution is achieved. To our knowledge, H2RBox-v2 is the first symmetry-supervised paradigm for oriented object detection. Compared to H2RBox, our method is less susceptible to low annotation quality and insufficient training data, which in such cases is expected to give a competitive performance much closer to fully-supervised oriented object detectors. Specifically, the performance comparison between H2RBox-v2 and Rotated FCOS on DOTA-v1.0/1.5/2.0 is 72.31%/64.76%/50.33% vs. 72.44%/64.53%/51.77%, 89.66% vs. 88.99% on HRSC, and 42.27% vs. 41.25% on FAIR1M.

1 Introduction

Object detection has been studied extensively, with early research focusing mainly on horizontal detection [1, 2]. When fine-grained bounding boxes are required, oriented object detection [3] is considered more preferable, especially in complex scenes such as aerial images [4–8], scene text [9–13], retail scenes [14], and industrial inspection [15, 16].

With oriented object detection being featured, some horizontal-labeled datasets have been re-annotated, such as DIOR [17] to DIOR-R [18] for aerial image (192K instances) and SKU110K [19] to SKU110K-R [14] for retail scene (1,733K instances). Although re-annotation enables the training of oriented detectors, two facts cannot be ignored: **1)** Horizontal boxes (HBoxes) are still more readily available in existing datasets; **2)** Rotated box (RBox) or Mask annotation are labor-intensive and more expensive than the horizontal one.

*Equal contribution

†Correspondence author

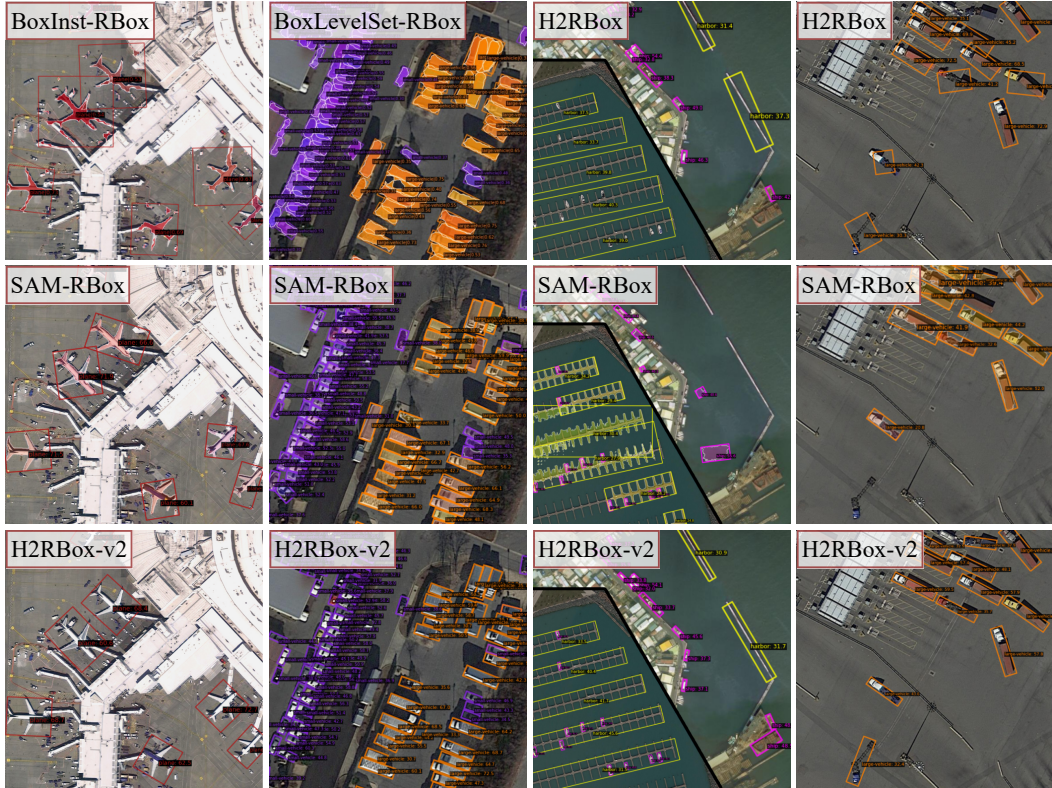


Figure 1: Visual comparisons of HBox-supervised oriented detectors, including BoxInst-RBox (2021) [21], BoxLevelSet-RBox (2022) [22], H2RBox (2023) [20] in the first row, SAM-RBox (2023) [23] in the second row, and H2RBox-v2 in the third row.

Such a situation raises an interesting question: Can we achieve oriented object detection directly under the weak supervision of HBox annotation? Yang et al. [20] explored this new task setting and proposed the first general solution called HBox-to-RBox (H2RBox) in 2023.

H2RBox gives an effective paradigm and outperforms potential alternatives, including HBox-Mask-RBox (generating RBoxes from segmentation mask) powered by BoxInst [21] and BoxLevelSet [22], the state-of-the-art HBox-supervised instance segmentation methods. But yet, it is not impeccable:

- 1) H2RBox learns the angle from the geometry of circumscribed boxes, requiring high annotation quality and a large number of training data containing the same object in various orientations.
- 2) H2RBox requires quite restrictive working conditions. For example, it is incompatible with rotation augmentation and is sensitive to black borders on images.

If the above requirements are not met, H2RBox may perform far below expectations. As a result, H2RBox does not support some small datasets (e.g. HRSC [5]) and some augmentation methods (e.g. random rotation), leading to bottlenecks in its application scenarios and performance.

By rethinking HBox-supervised oriented object detection with a powerful yet unexplored theory, symmetry-based self-supervision, we present H2RBox-v2, a new version of H2RBox that exploits the symmetry of objects and solves the above issues.

Motivations of this paper: Symmetry is a natural property widespread in various scenes. For example, in the DOTA dataset [4], many categories (planes, courts, vehicles, ships, etc.) show significant axial symmetry. During RBox annotation, symmetry is also an important consideration—Humans can intuitively take the direction of the symmetrical axis as the orientation, even without annotation guidance. Therefore, symmetry supervision for angle prediction is theoretically feasible. Is there a way to use symmetry as a supervising tool in deep neural networks for oriented object detection? Will this technique lead to better performance? These are the questions for which this paper is intended.

What is new in H2RBox-v2? **1)** A new self-supervised branch leaning angle from symmetry. H2RBox-v2 directly learns angles from the image through the symmetry of objects. That means it is capable of learning the angles correctly even if the HBox annotations are inaccurate in size (not precisely the bounding rectangle) or when the training data is relatively insufficient. **2)** A newly designed CircumIoU loss in the weakly-supervised branch. With this amendment, H2RBox-v2 is now compatible with random rotation augmentation. **3)** As a result, H2RBox-v2 gives a higher performance (as is displayed in Figure 1), further bridging the gap between HBox-supervised and RBox-supervised oriented object detection.

Contributions of this paper: **1)** This work is the first attempt to explore symmetry supervision for angle regression in oriented object detection and to empirically show that symmetry in images can help the deep neural network learn the orientation of objects in a self-supervised manner. **2)** A new training paradigm upon symmetry supervision is elaborated on, and an integral and stable implementation is provided in this paper. Most importantly, the codes are well-written, reproducible, and publicly available. **3)** The performance of the proposed methods is evaluated through extensive experiments, proving that the proposed method is capable of learning the orientation from symmetry, resulting in a performance higher than H2RBox, the current state-of-the-art.

The rest of this paper is organized as: Section 2 reviews the related methods around oriented object detection. Section 3 describes the methods in detail. Section 4 conducts experiments on several datasets to evaluate the performance. Section 5 concludes the paper.

2 Related Work

RBox-supervised oriented object detection: Extensive studies around supervised oriented object detection have been carried out, among which representative ones include anchor-based detector Rotated RetinaNet [24], anchor-free detector Rotated FCOS [25], and two-stage detectors such as RoI Transformer [26], Oriented R-CNN [27] and ReDet [28]. Besides, R³Det [29] and S²A-Net [30] improve the performance by exploiting alignment features.

Most of the above methods directly perform angle regression, which may face loss discontinuity and regression inconsistency induced by the periodicity of the angle. Several studies are thus carried out for such issues, including modulated losses [31, 32] that alleviate loss jumps, angle coders [33–35] that convert the angle into boundary-free coded data, and Gaussian-based losses [36–39] that transform rotated bounding boxes into Gaussian distributions.

Additionally, RepPoint-based methods [40–42] provide new alternatives for oriented object detection, which predict a set of sample points that bounds the spatial extent of an object.

HBox-supervised instance segmentation: Compared with HBox-supervised oriented object detection, HBox-supervised instance segmentation, a similar task also belonging to weakly-supervised learning, has been better studied in the literature. For instance, SDI [43] refines the segmentation through an iterative training process; BBTP [44] formulates the HBox-supervised instance segmentation into a multiple-instance learning problem based on Mask R-CNN [45]; BoxInst [21] uses the color-pairwise affinity with box constraint under an efficient RoI-free CondInst [46]; BoxLevelSet [22] introduces an energy function to predict the instance-aware mask as the level set; SAM (Segment Anything Model) [23] produces object masks from input prompts such as points or HBoxes.

Most importantly, these HBox-supervised instance segmentation methods are potentially applicable to HBox-supervised oriented object detection by finding the minimum circumscribed rectangle of the segmentation mask. Such an HBox-Mask-RBox paradigm is a potential alternative for the task we are aiming at and is thus added to our experiments for comparison.

HBox-supervised oriented object detection: Though the oriented bounding box can be obtained from the segmentation mask, such an HBox-Mask-RBox pipeline is much more complex and with limited performance in both speed and accuracy. To skip the segmentation step and achieve RBox detection directly from HBox annotation, H2RBox [20] is proposed. With HBox annotations for the same object in various orientations, the geometric constraint limits the object to several candidate angles. Supplemented with a self-supervised branch eliminating the undesired results, an HBox-to-RBox paradigm is built.

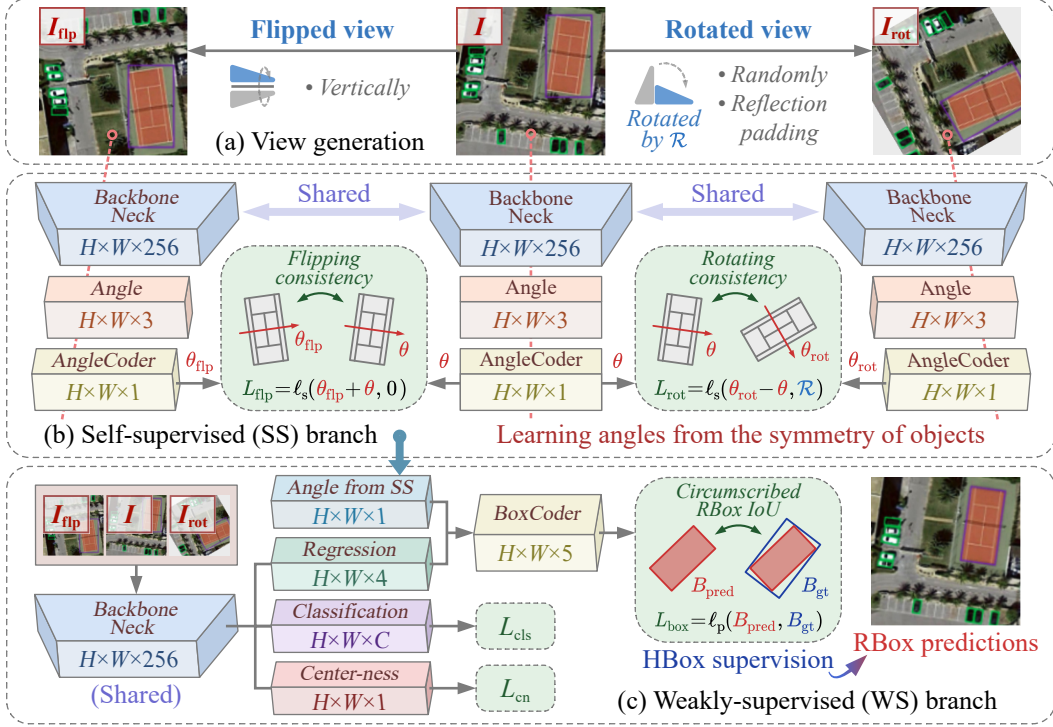


Figure 2: The overview of H2RBox-v2, consisting of a self-supervised branch that learns angles from the symmetry of objects, and a weakly-supervised branch that learns other properties from HBoxes.

Some similar studies use additional annotated data for training, which are also attractive but less general than H2RBox: **1)** OAOD [47] is proposed for weakly-supervised oriented object detection. But in fact, it uses HBox along with an object angle as annotation, which is just “slightly weaker” than RBox supervision. Such an annotation manner is not commonly used, and thus OAOD is only verified on their self-collected ITU Firearm dataset. **2)** KCR [48] combines RBox-annotated source datasets with HBox-annotated target datasets, and achieves HBox-supervised oriented detection on the target datasets through transfer learning. **3)** Another solution WSODet [49], also proposed in 2023, achieves HBox-supervised oriented detection by generating pseudo orientation labels from the feature map but is significantly worse than H2RBox. To conclude, H2RBox is still the most competitive method among all alternatives at present.

3 Proposed Method

An overview of H2RBox-v2 is given in Figure 2, which consists of a self-supervised branch (Section 3.2) and a weakly-supervised branch (Section 3.3). The symmetry principles that form the basis of the self-supervised branch are described in Section 3.1.

3.1 Basic Definitions and Principles

Definition of axisymmetry: An image I is axisymmetric if, after being flipped along a line, it can overlap with the original image, and this line is called the axis of symmetry.

Assume there is a neural network $f_{nn}(\cdot)$ that maps an axisymmetric image I to a real number θ :

$$\theta = f_{nn}(I) \quad (1)$$

To exploit axisymmetry for deep learning, we endow the function with two new properties: flipping consistency and rotating consistency.

Flipping consistency: With an input image vertically flipped, $f_{nn}(\cdot)$ gives an opposite output:

$$f_{nn}(I) + f_{nn}(\text{flip}(I)) = 0 \quad (2)$$

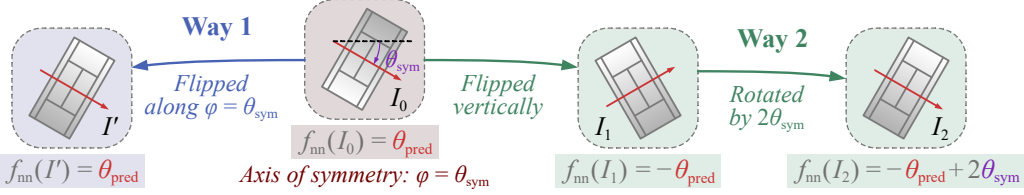


Figure 3: To illustrate that the axisymmetry (Way 1) is equivalent to a vertical flip plus a rotation (Way 2). The expected outputs at the bottom show that $f_{\text{nn}}(I') = f_{\text{nn}}(I_2) \Rightarrow \theta_{\text{pred}} = \theta_{\text{sym}}$.

where $\text{flip}(I)$ is an operator of vertically flipping the image I .

Rotating consistency: With an input rotated by \mathcal{R} , the output of $f_{\text{nn}}(\cdot)$ also increases by \mathcal{R} :

$$f_{\text{nn}}(\text{rot}(I, \mathcal{R})) - f_{\text{nn}}(I) = \mathcal{R} \quad (3)$$

where $\text{rot}(I, \mathcal{R})$ is an operator that clockwise rotates the image I by \mathcal{R} .

Main reasoning: Given an image I_0 axisymmetric along $\varphi = \theta_{\text{sym}}$, assuming the corresponding output is $\theta_{\text{pred}} = f_{\text{nn}}(I_0)$, the image can be transformed in two ways as shown in Figure 3:

- **Way 1:** Flipping I_0 along line $\varphi = \theta_{\text{sym}}$. According to the above definition of axisymmetry, the output remains the same, i.e. $f_{\text{nn}}(I') = f_{\text{nn}}(I_0) = \theta_{\text{pred}}$.
- **Way 2:** Flipping I_0 vertically to obtain I_1 first, and then rotating I_1 by $2\theta_{\text{sym}}$ to obtain I_2 . According to flipping and rotating consistencies, the output is supposed to be $f_{\text{nn}}(I_2) = -\theta_{\text{pred}} + 2\theta_{\text{sym}}$.

On the ground that ways 1 and 2 are equivalent, the transformed images I' and I_2 are identical. And thus $f_{\text{nn}}(I') = f_{\text{nn}}(I_2)$, finally leading to $\theta_{\text{pred}} = \theta_{\text{sym}}$.

Thereby, a conclusion can be drawn: If image I_0 is axisymmetric along line $\varphi = \theta_{\text{sym}}$ and function $f_{\text{nn}}(\cdot)$ subjects to both flipping and rotating consistencies, then $f_{\text{nn}}(I_0)$ must be equal to θ_{sym} .

Limitations of the above reasoning: 1) For higher conciseness, the periodicity is not included. To allow images to be rotated into another cycle, the consistencies should be modified as:

$$\begin{aligned} f_{\text{nn}}(I) + f_{\text{nn}}(\text{flip}(I)) &= k\pi \\ f_{\text{nn}}(\text{rot}(I, \mathcal{R})) - f_{\text{nn}}(I) &= \mathcal{R} + k\pi \end{aligned} \quad (4)$$

where k is an integer to keep left and right in the same cycle. This problem is coped with using Snap loss in Section 3.4. Meanwhile, the conclusion should be amended as: $f_{\text{nn}}(I_0) = \theta_{\text{sym}} + k\pi/2$, meaning that the network outputs either the axis of symmetry or a perpendicular one.

2) Image I_0 contains only one axisymmetric object. Nevertheless, the experiments demonstrate that the above principles are also applicable for multiple object detection with objects not perfectly axisymmetric, where an approximate axis of each object can be found through deep learning.

3.2 Self-supervised (SS) Branch

The above analysis suggests that the network can learn the angle of objects from symmetry through the flipping and rotating consistencies. A self-supervised branch is accordingly designed.

During the training process, we perform vertical flip and random rotation to generate two transformed views, I_{flip} and I_{rot} , of the input image I , as shown in Figure 2 (a). The blank border area induced by rotation is filled with reflection padding. Afterward, the three views are fed into three parameter-shared branches of the network, where ResNet50 [50] and FPN [51] are used as the backbone and the neck, respectively. The random rotation is in range $\pi/4 \sim 3\pi/4$ (according to Table 6).

Similar to H2RBox, a label assigner is required in the SS branch to match the objects in different views. In H2RBox-v2, we calculate the average angle features on all sample points for each object and eliminate those objects without correspondence (some objects may be lost during rotation).

Following the assigner, an angle coder PSC [35] is further adopted in H2RBox-v2 to cope with the boundary problem and improve the stability and performance (as verified in Table 3). The outputs of the original, flipped, and rotated views are denoted as θ , θ_{flip} , and θ_{rot} , respectively.

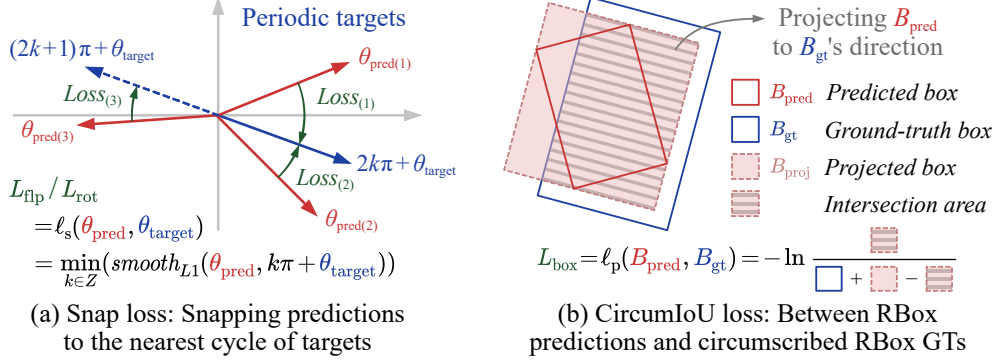


Figure 4: Illustration of the Snap loss (for SS branch) and the CircumIoU loss (for WS branch).

Finally, with formula in Section 3.4, the loss L_{flip} can be calculated between θ and θ_{flip} , whereas L_{rot} between θ and θ_{rot} . By minimizing L_{flip} and L_{rot} , the network learns to conform with flipping and rotating consistencies and gains the ability of angle prediction through self-supervision.

3.3 Weakly-supervised (WS) Branch

The SS branch above provides the angle of objects. To predict other properties of the bounding box (position, size, category, etc.), a weakly-supervised branch using HBox supervision is further introduced. The WS branch in H2RBox-v2 is inherited from H2RBox, but has some differences:

- 1) In H2RBox, the angle is primarily learned by the WS branch, with an SS branch eliminating the undesired results. Comparably, H2RBox-v2 has a powerful SS branch driven by symmetry that can learn the angle independently, and thus the angle subnet is deleted from the WS branch.
- 2) H2RBox converts B_{pred} to an Hbox to calculate the IoU loss [52] with the HBox B_{gt} , which cannot work with random rotation where B_{gt} becomes an RBox. To solve this problem, CircumIoU loss (detailed in Section 3.4) is proposed in H2RBox-v2 to directly calculate L_{box} between B_{pred} and B_{gt} , so that B_{gt} is allowed to be an RBox circumscribed to B_{pred} , as is shown in Figure 2 (c).

3.4 Loss Functions

Loss for SS branch: As is described in Equation (4), the consistencies encounter the periodicity problem in rotation. To cope with this problem, Snap loss ℓ_s is proposed in this paper as:

$$\ell_s(\theta_{\text{pred}}, \theta_{\text{target}}) = \min_{k \in \mathbb{Z}} (\text{smooth}_{L1}(\theta_{\text{pred}}, k\pi + \theta_{\text{target}})) \quad (5)$$

where an illustration is displayed in Figure 4 (a). The Snap loss is used in both L_{flip} and L_{rot} as:

$$\begin{aligned} L_{\text{flip}} &= \ell_s(\theta_{\text{flip}} + \theta, 0) \\ L_{\text{rot}} &= \ell_s(\theta_{\text{rot}} - \theta, \mathcal{R}) \end{aligned} \quad (6)$$

where L_{flip} is the loss for flipping consistency, and L_{rot} for rotating consistency. θ , θ_{flip} , and θ_{rot} are the outputs of the three views described in Section 3.2. \mathcal{R} is the angle in generating rotated view.

With the above definitions, the loss of the SS branch can be expressed as:

$$L_{\text{ss}} = \lambda L_{\text{flip}} + L_{\text{rot}} \quad (7)$$

where λ is the weight set to 0.05 according to the ablation study in Table 5.

Loss for WS branch: The losses in the WS branch are mainly defined by the backbone FCOS detector, including L_{cls} for classification and L_{cn} for center-ness. Different from RBox-supervised methods, B_{gt} in H2RBox-v2 is an RBox circumscribed to B_{pred} , so we re-define the loss for box regression L_{box} with CircumIoU loss, which is demonstrated in Figure 4 (b).

The loss of the WS branch can be expressed as:

$$L_{\text{ws}} = \mu_1 L_{\text{cls}} + \mu_2 L_{\text{cn}} + \mu_3 L_{\text{box}} \quad (8)$$

Table 1: Results on the DOTA-v1.0 dataset.

	Method	Sched.	MS	RR	Size	FPS	AP ₅₀
RBox-supervised	RepPoints (2019) [40]	1x			1024	24.5	68.45
	RetinaNet (2017) [24]	1x			1024	25.4	68.69
	GWD (2021) [36]	1x			1024	25.4	71.66
	KFIoU (2023) [39]	1x			1024	25.4	71.61
	KLD (2021) [37]	1x			1024	25.4	71.24
	PSC (2023) [35]	1x			1024	25.4	71.92
	SASM (2022) [56]	1x			1024	24.4	72.30
	R ³ Det (2021) [29]	1x			1024	20.0	73.12
	CFA (2021) [57]	1x			1024	24.5	73.84
	Oriented RepPoints (2022) [42]	1x			1024	24.5	75.26
	S ² A-Net (2022) [30]	1x			1024	23.3	75.81
	FCOS (2019) [25]	1x			1024	29.5	72.44
	FCOS (2019) [25]	3x		✓	1024	29.5	74.75
	FCOS (2019) [25]	1x	✓	✓	1024	29.5	77.68
HBox-supervised	BoxInst-RBox (2021) [21] ¹	1x			960	2.7	53.59
	BoxLevelSet-RBox (2022) [22] ²	1x			960	4.7	56.44
	SAM-ViT-B-RBox (2023) [23] ³	1x			1024	1.7	63.94
	H2RBox (FCOS-based) (2023) [20] ⁴	1x			1024	29.1	67.82
	H2RBox (FCOS-based) (2023) [20] ⁵	1x			1024	29.1	70.05
	H2RBox-v2 (FCOS-based)	1x			960	31.6	71.46
	H2RBox-v2 (FCOS-based)	1x			1024	29.1	72.31
	H2RBox-v2 (FCOS-based)	3x		✓	1024	29.1	74.29
	H2RBox-v2 (FCOS-based)	1x	✓		1024	29.1	77.97
	H2RBox-v2 (FCOS-based)	1x	✓	✓	1024	29.1	78.25
	H2RBox-v2 (FCOS-based, Swin-T) ⁶	1x	✓	✓	1024	24.0	79.19
	H2RBox-v2 (FCOS-based, Swin-B) ⁶	1x	✓	✓	1024	12.4	79.75

¹ “-RBox” means the minimum rectangle operation is performed on the Mask to obtain RBox.

² Evaluated on NVIDIA V100 GPU due to the excessive RAM usage.

³ The code is available at <https://github.com/Li-Qingyun/sam-mmrotate>.

⁴ Results reported in the original paper. ⁵ Results reproduced by us with fair infrastructure.

⁶ Using Swin Transformer [58] as backbone.

where the hyper-parameters are set to $\mu_1 = 1$, $\mu_2 = 1$, and $\mu_3 = 1$ by default.

Overall loss: The overall loss of the proposed network is the sum of the WS loss and the SS loss:

$$L_{\text{total}} = L_{\text{ws}} + L_{\text{ss}} \quad (9)$$

4 Experiments

Using PyTorch 1.13.1 [53] and MMRotate 1.0.0 [54] tool kits, experiments are carried out to evaluate the performance. We also implement a version via Jittor [55]. The listed results are obtained on the same platforms (PyTorch/MMRotate version) with the same hyper-parameters (learning rate, batch size, optimizer, etc.).

4.1 Datasets and Settings

DOTA [4]: DOTA is comprised of 2,806 large aerial images—1,411 for training, 937 for validation, and 458 for testing. The dataset is annotated using 15 categories with 188,282 instances in total. The categories are defined as: Plane (PL), Baseball Diamond (BD), Bridge (BR), Ground Field Track (GTF), Small Vehicle (SV), Large Vehicle (LV), Ship (SH), Tennis Court (TC), Basketball Court (BC), Storage Tank (ST), Soccer-Ball Field (SBF), Roundabout (RA), Harbor (HA), Swimming Pool (SP), and Helicopter (HC). We follow the standard preprocessing procedure in MMRotate—The high-resolution images are split into $1,024 \times 1,024$ patches with an overlap of 200 pixels for training, and the detection results of all patches are merged to evaluate the performance.

Table 2: AP₅₀ performance on the DOTA-v1.5, DOTA-v2.0, HRSC, and FAIR1M datasets.

Method	DOTA-v1.5	DOTA-v2.0	HRSC	FAIR1M
RetinaNet (2017) [24]	60.57	47.00	84.49	37.67
GWD (2021) [36]	63.27	48.87	86.67	39.11
S ² A-Net (2022) [30]	66.53	52.39	90.10	42.44
FCOS (2019) [25]	64.53	51.77	88.99	41.25
KCR (2023) [48]*	-	-	79.10	-
H2RBox (FCOS-based) (2023) [20]	61.70	48.68	7.03	35.94
H2RBox-v2 (FCOS-based)	64.76	50.33	89.66	42.27

* Transfer learning from DOTA (RBox) to HRSC (HBox). The result is cited from their paper.

HRSC [5]: As a ship detection dataset, HRSC contains ship instances both on the sea and inshore, with arbitrary orientation. The training, validation, and testing set include 436, 181, and 444 images, respectively. We use the preprocessing provided by MMRotate, where the images are scaled to 800×800 for training and testing.

FAIR1M [59]: FAIR1M is a benchmark dataset with more than 1 million instances and more than 40,000 images for fine-grained object recognition in high-resolution remote sensing imagery. The dataset is annotated with five categories and 37 fine-grained subcategories. We split the images into $1,024 \times 1,024$ patches with an overlap of 200 pixels and a scale rate of 1.5 and merge the results for testing. The performance is evaluated on the FAIR1M-1.0 server.

Experimental settings: We adopt the FCOS [25] detector with ResNet50 [50] backbone and FPN [51] neck as the baseline method, based on which we develop our H2RBox-v2. We choose average precision (AP) as the primary metric to compare with existing literature. For a fair comparison, all the listed models are configured based on ResNet50 [50] backbone and trained on NVIDIA RTX3090/4090 GPUs. All models are trained with AdamW [60], with an initial learning rate of $5e-5$ and a mini-batch size of 2. Besides, we adopt a learning rate warm-up for 500 iterations, and the learning rate is divided by ten at each decay step. “1x”, “3x”, and “6x” schedules indicate 12, 36, and 72 epochs for training. “MS” and “RR” denote multi-scale technique [54] and random rotation augmentation. Unless otherwise specified, “6x” is used for HRSC and “1x” for the other datasets, while random flipping is the only augmentation that is always adopted by default.

4.2 Main Results

DOTA-v1.0: The results in Table 1 demonstrate that H2RBox-v2 outperforms the HBox-Mask-Rbox framework by a large margin in both accuracy and speed. Taking BoxLevelSet-RBox [22] as an example, H2RBox-v2 gives an accuracy of 15.02% higher, and a speed about 7 times faster due to the time-consuming post-processing (i.e. minimum circumscribed rectangle operation). Recently, SAM [23] has demonstrated strong zero-shot capabilities by training on the largest segmentation dataset to date. Thus, we use a trained horizontal FCOS detector to provide HBoxes into SAM as prompts, so that corresponding Masks can be generated by zero-shot, and finally the rotated RBoxes are obtained by performing the minimum circumscribed rectangle operation on the predicted Masks. Thanks to the powerful zero-shot capability, SAM-RBox based on ViT-B [61] in Table 1 has achieved 63.94%. However, it is also limited to the additional mask prediction step and the time-consuming post-processing, only 1.7 FPS during inference.

In comparison with the current state-of-the-art method H2RBox, to make it fair, we use the reproduced result of H2RBox, which achieves 70.05%, 2.23% higher than the original paper [20]. In this fair comparison, our method outperforms H2RBox by 2.26% (72.31% vs. 70.05%).

Furthermore, the performance gap between our method and the RBox-supervised FCOS baseline is only 0.13% and 0.46% (with RR augmentation). When MS and RR are both applied, our method outperforms RBox-supervised FCOS by 0.57% (78.25% vs. 77.68%), proving that supplemented with the supervision from symmetry, the weakly-supervised learning can achieve performance on a par with the fully-supervised one upon the same neural network. Finally, H2RBox-v2 obtains 79.75% on DOTA-v1.0 by further utilizing a stronger backbone.

Table 3: Ablation with different SS losses.

Dataset	PSC	ℓ_s	AP	AP ₅₀	AP ₇₅
DOTA		✓	24.24	52.24	19.48
		✓	0.01	0.77	0.02
	✓		10.49	27.57	6.15
	✓	✓	40.69	72.31	39.49
HRSC			2.25	7.83	0.62
		✓	48.95	88.52	50.03
	✓		0.31	0.88	0.13
	✓	✓	58.03	89.66	64.80

Table 4: Ablation with different WS losses.

Dataset	ℓ_p	RR	AP	AP ₅₀	AP ₇₅
DOTA			39.35	71.49	37.03
		✓	11.93	29.34	7.86
	✓		40.69	72.31	39.49
	✓	✓	40.17	71.79	39.77
HRSC			56.20	89.58	61.84
		✓	41.10	87.19	33.97
	✓		58.03	89.66	64.80
	✓	✓	63.82	89.56	76.11

Table 5: Ablation with different weights between L_{fp} and L_{rot} .

Dataset	λ	AP	AP ₅₀	AP ₇₅	Dataset	λ	AP	AP ₅₀	AP ₇₅
DOTA	0.01	40.43	72.26	38.55	HRSC	0.01	55.78	89.20	61.72
	0.05	40.39	72.59	39.18		0.05	56.76	89.63	62.93
	0.1	40.48	71.46	39.84		0.1	58.22	89.45	64.99
	0.5	39.94	72.26	38.16		0.5	53.85	88.90	61.47
	1.0	38.50	70.91	36.02		1.0	1.57	6.97	0.38

Table 6: Ablation with different random ranges in the rotated view generation on HRSC.

Range	AP	AP ₅₀	AP ₇₅
$-\pi \sim \pi^*$	56.57	89.47	63.14
$\pi/4 \sim 3\pi/4$	58.22	89.45	64.99
$3\pi/8 \sim 5\pi/8$	56.81	89.83	64.03
$7\pi/16 \sim 9\pi/16$	55.56	89.40	61.28

* Not stable, occasionally be much lower.

Table 7: Ablation with different padding strategies for rotated view generation.

Dataset	Padding	AP	AP ₅₀	AP ₇₅
DOTA	Zeros	40.49	72.26	39.15
	Reflection	40.69	72.31	39.49
HRSC	Zeros	55.90	89.32	60.95
	Reflection	58.03	89.66	64.80

DOTA-v1.5/2.0: As extended versions of DOTA-v1.0, these two datasets are more challenging, while the results present a similar trend. Still, H2RBox-v2 shows considerable advantages over H2RBox, with an improvement of 3.06% on DOTA-v1.5 and 1.65% on DOTA-v2.0. The results on DOTA-v1.5/2.0, HRSC, and FAIR1M are shown in Table 2.

HRSC: H2RBox can hardly learn angle information from small datasets like HRSC, resulting in deficient performance. Contrarily, H2RBox-v2 is good at this kind of task, giving a performance comparable to fully-supervised methods. Compared to KCR [48] that uses transfer learning from RBox-supervised DOTA to HBox-supervised HRSC, our method, merely using HBox-supervised HRSC, outperforms KCR by 10.56% (89.66% vs. 79.10%).

FAIR1M: This dataset contains a large number of planes, vehicles, and courts, which are more perfectly axisymmetric than objects like bridges and harbors in DOTA. This may explain the observation that H2RBox-v2, supervised by symmetry, outperforms H2RBox by a more considerable margin of 6.33% (42.27% vs. 35.94%). In this case, H2RBox-v2 even performs superior to the fully-supervised FCOS that H2RBox-v2 is based on by 1.02% (42.27% vs. 41.25%).

4.3 Ablation Studies

Loss in SS branch: Table 3 studies the impact of 1) using Snap loss or SmoothL1 loss, 2) using angle coder or not in the SS branch. Column “ ℓ_s ” denotes using Snap loss introduced in Section 3.4, and column “PSC” indicates using PSC angle coder [35] before calculating the loss. These two modules are designed to cope with the periodicity of the angle, and the results prove that both modules are essential for H2RBox-v2 to achieve a stable and high-performance solution.

Loss in WS branch: Table 4 demonstrates that CircumIoU loss can work with random rotation to further improve the performance, which H2RBox is incapable of. The checkmark in “ ℓ_p ” means

using CircumIoU loss introduced in Section 3.4, and otherwise, IoU loss [52] is used following a conversion from RBox to HBox (the manner of H2RBox [20]).

Weights between L_{flip} and L_{rot} : Table 5 shows that on both DOTA and HRSC datasets, $\lambda = 0.05$ could be the best choice under AP_{50} metric, whereas $\lambda = 0.1$ under AP_{75} . Hence in most experiments, we choose $\lambda = 0.05$, except for Table 6 where $\lambda = 0.1$ is used.

Range of view generation: When the rotation angle \mathcal{R} is close to 0, the SS branch could fall into a sick state. This may explain the fluctuation of losses under the random rotation within $-\pi \sim \pi$, leading to training instability. According to Table 6, $\pi/4 \sim 3\pi/4$ is more suitable, accelerating the convergence in the early stages and leading to higher performance in the end.

Padding strategies: Compared to the performance loss of more than 10% for H2RBox without reflection padding, Table 7 shows that H2RBox-v2 is less sensitive to black borders.

5 Conclusion

This paper presents H2RBox-v2, a weakly-supervised detector that learns the RBox from the HBox annotation. Unlike the previous version H2RBox, H2RBox-v2 learns the angle directly from the image of the objects through a powerful symmetry-driven self-supervised branch, which further bridges the gap between HBox-supervised and RBox-supervised oriented object detection.

Extensive experiments are then carried out, from which the following conclusions can be drawn:

- 1) Compared to H2RBox, H2RBox-v2 achieves higher accuracy on various datasets, with an improvement of 2.32% on average over three versions of DOTA, and 6.33% on the FAIR1M dataset.
- 2) H2RBox-v2 is less susceptible to low annotation quality and insufficient training data. As a result, it is compatible with small datasets such as HRSC, which H2RBox cannot handle.
- 3) Even when compared to fully-supervised methods, H2RBox-v2 still shows quite competitive performance, proving the effectiveness and the potentiality of symmetry supervision.

References

- [1] Zhong-Qiu Zhao, Peng Zheng, Shou-Tao Xu, and Xindong Wu. Object detection with deep learning: A review. *IEEE Transactions on Neural Networks and Learning Systems*, 30(11):3212–3232, 2019.
- [2] Li Liu, Wanli Ouyang, Xiaogang Wang, Paul Fieguth, Jie Chen, Xinwang Liu, and Matti Pietikäinen. Deep learning for generic object detection: A survey. *International Journal of Computer Vision*, 128(2):261–318, 2020.
- [3] Long Wen, Yu Cheng, Yi Fang, and Xinyu Li. A comprehensive survey of oriented object detection in remote sensing images. *Expert Systems with Applications*, page 119960, 2023.
- [4] Gui-Song Xia, Xiang Bai, Jian Ding, Zhen Zhu, Serge Belongie, Jiebo Luo, Mihai Datcu, Marcello Pelillo, and Liangpei Zhang. DOTA: A large-scale dataset for object detection in aerial images. In *IEEE/CVF Conference on Computer Vision and Pattern Recognition*, pages 3974–3983, 2018.
- [5] Zikun Liu, Liu Yuan, Lubin Weng, and Yiping Yang. A high resolution optical satellite image dataset for ship recognition and some new baselines. In *Proceedings of the International Conference on Pattern Recognition Applications and Methods*, volume 2, pages 324–331, 2017.
- [6] Xue Yang, Hao Sun, Kun Fu, Jirui Yang, Xian Sun, Menglong Yan, and Zhi Guo. Automatic ship detection in remote sensing images from google earth of complex scenes based on multiscale rotation dense feature pyramid networks. *Remote Sensing*, 10(1), 2018.
- [7] Xue Yang and Junchi Yan. On the arbitrary-oriented object detection: Classification based approaches revisited. *International Journal of Computer Vision*, 130:1340–1365, 2022.
- [8] Kun Fu, Zhonghan Chang, Yue Zhang, Guangluan Xu, Keshu Zhang, and Xian Sun. Rotation-aware and multi-scale convolutional neural network for object detection in remote sensing images. *ISPRS Journal of Photogrammetry and Remote Sensing*, 161:294–308, 2020.

- [9] Nibal Nayef, Fei Yin, Imen Bizid, Hyunsoo Choi, Yuan Feng, Dimosthenis Karatzas, Zhenbo Luo, Umapada Pal, Christophe Rigaud, Joseph Chazalon, Wafa Khelif, Muhammad Muzzamil Luqman, Jean-Christophe Burie, Cheng-lin Liu, and Jean-Marc Ogier. Icdar2017 robust reading challenge on multi-lingual scene text detection and script identification - rrc-mlt. In *IAPR International Conference on Document Analysis and Recognition*, volume 01, pages 1454–1459, 2017.
- [10] Jianqi Ma, Weiyuan Shao, Hao Ye, Li Wang, Hong Wang, Yingbin Zheng, and Xiangyang Xue. Arbitrary-oriented scene text detection via rotation proposals. *IEEE Transactions on Multimedia*, 20(11):3111–3122, 2018.
- [11] Minghui Liao, Zhen Zhu, Baoguang Shi, Gui-Song Xia, and Xiang Bai. Rotation-sensitive regression for oriented scene text detection. In *IEEE/CVF Conference on Computer Vision and Pattern Recognition*, pages 5909–5918, 2018.
- [12] Xuebo Liu, Ding Liang, Shi Yan, Dagui Chen, Yu Qiao, and Junjie Yan. Fots: Fast oriented text spotting with a unified network. In *IEEE/CVF Conference on Computer Vision and Pattern Recognition*, pages 5676–5685, 2018.
- [13] Xinyu Zhou, Cong Yao, He Wen, Yuzhi Wang, Shuchang Zhou, Weiran He, and Jiajun Liang. East: An efficient and accurate scene text detector. In *IEEE Conference on Computer Vision and Pattern Recognition*, pages 2642–2651, 2017.
- [14] Xingjia Pan, Yuqiang Ren, Kekai Sheng, Weiming Dong, Haolei Yuan, Xiaowei Guo, Chongyang Ma, and Changsheng Xu. Dynamic refinement network for oriented and densely packed object detection. In *IEEE/CVF Conference on Computer Vision and Pattern Recognition*, pages 11207–11216, 2020.
- [15] Yuekai Liu, Hongli Gao, Liang Guo, Aoping Qin, Canyu Cai, and Zhichao You. A data-flow oriented deep ensemble learning method for real-time surface defect inspection. *IEEE Transactions on Instrumentation and Measurement*, 69(7):4681–4691, 2020.
- [16] Hongjin Wu, Ruoshan Lei, and Yibing Peng. Pcbnet: A lightweight convolutional neural network for defect inspection in surface mount technology. *IEEE Transactions on Instrumentation and Measurement*, 71:1–14, 2022.
- [17] Ke Li, Gang Wan, Gong Cheng, Liqiu Meng, and Junwei Han. Object detection in optical remote sensing images: A survey and a new benchmark. *ISPRS Journal of Photogrammetry and Remote Sensing*, 159:296–307, 2020.
- [18] Gong Cheng, Jiabao Wang, Ke Li, Xingxing Xie, Chunbo Lang, Yanqing Yao, and Junwei Han. Anchor-free oriented proposal generator for object detection. *IEEE Transactions on Geoscience and Remote Sensing*, 2022.
- [19] Eran Goldman, Roei Herzig, Aviv Eisenschtat, Jacob Goldberger, and Tal Hassner. Precise detection in densely packed scenes. In *IEEE/CVF Conference on Computer Vision and Pattern Recognition*, pages 5227–5236, 2019.
- [20] Xue Yang, Gefan Zhang, Wentong Li, Xuehui Wang, Yue Zhou, and Junchi Yan. H2rbox: Horizontal box annotation is all you need for oriented object detection. *International Conference on Learning Representations*, 2023.
- [21] Zhi Tian, Chunhua Shen, Xinlong Wang, and Hao Chen. Boxinst: High-performance instance segmentation with box annotations. In *IEEE/CVF Conference on Computer Vision and Pattern Recognition*, pages 5443–5452, 2021.
- [22] Wentong Li, Wenyu Liu, Jianke Zhu, Miaomiao Cui, Xiansheng Hua, and Lei Zhang. Box-supervised instance segmentation with level set evolution. In *European Conference on Computer Vision*, 2022.
- [23] Alexander Kirillov, Eric Mintun, Nikhila Ravi, Hanzi Mao, Chloe Rolland, Laura Gustafson, Tete Xiao, Spencer Whitehead, Alexander C. Berg, Wan-Yen Lo, Piotr Dollár, and Ross Girshick. Segment anything. *arXiv:2304.02643*, 2023.
- [24] Tsung-Yi Lin, Priya Goyal, Ross Girshick, Kaiming He, and Piotr Dollár. Focal loss for dense object detection. *IEEE Transactions on Pattern Analysis and Machine Intelligence*, 42(2):318–327, 2020.
- [25] Zhi Tian, Chunhua Shen, Hao Chen, and Tong He. Fcos: Fully convolutional one-stage object detection. In *IEEE/CVF International Conference on Computer Vision*, pages 9626–9635, 2019.

- [26] Jian Ding, Nan Xue, Yang Long, Gui-Song Xia, and Qikai Lu. Learning roi transformer for oriented object detection in aerial images. In *IEEE/CVF Conference on Computer Vision and Pattern Recognition*, pages 2849–2858, 2019.
- [27] Xingxing Xie, Gong Cheng, Jiabao Wang, Xiwen Yao, and Junwei Han. Oriented r-cnn for object detection. In *IEEE/CVF International Conference on Computer Vision*, pages 3520–3529, 2021.
- [28] Jiaming Han, Jian Ding, Nan Xue, and Gui-Song Xia. Redet: A rotation-equivariant detector for aerial object detection. In *IEEE/CVF Conference on Computer Vision and Pattern Recognition*, pages 2785–2794, 2021.
- [29] Xue Yang, Junchi Yan, Ziming Feng, and Tao He. R3det: Refined single-stage detector with feature refinement for rotating object. In *Proceedings of the AAAI Conference on Artificial Intelligence*, volume 35, pages 3163–3171, 2021.
- [30] Jiaming Han, Jian Ding, Jie Li, and Gui-Song Xia. Align deep features for oriented object detection. *IEEE Transactions on Geoscience and Remote Sensing*, 60:1–11, 2022.
- [31] Xue Yang, Jirui Yang, Junchi Yan, Yue Zhang, Tengfei Zhang, Zhi Guo, Xian Sun, and Kun Fu. Scrdet: Towards more robust detection for small, cluttered and rotated objects. In *IEEE/CVF International Conference on Computer Vision*, pages 8231–8240, 2019.
- [32] Wen Qian, Xue Yang, Silong Peng, Junchi Yan, and Yue Guo. Learning modulated loss for rotated object detection. In *Proceedings of the AAAI Conference on Artificial Intelligence*, volume 35, pages 2458–2466, 2021.
- [33] Xue Yang and Junchi Yan. Arbitrary-oriented object detection with circular smooth label. In *European Conference on Computer Vision*, pages 677–694, 2020.
- [34] Xue Yang, Liping Hou, Yue Zhou, Wentao Wang, and Junchi Yan. Dense label encoding for boundary discontinuity free rotation detection. In *IEEE/CVF Conference on Computer Vision and Pattern Recognition*, pages 15814–15824, 2021.
- [35] Yi Yu and Feipeng Da. Phase-shifting coder: Predicting accurate orientation in oriented object detection. In *IEEE/CVF Conference on Computer Vision and Pattern Recognition*, 2023.
- [36] Xue Yang, Junchi Yan, Ming Qi, Wentao Wang, Xiaopeng Zhang, and Tian Qi. Rethinking rotated object detection with gaussian wasserstein distance loss. In *Proceedings of the 38th International Conference on Machine Learning*, volume 139, pages 11830–11841, 2021.
- [37] Xue Yang, Xiaojiang Yang, Jirui Yang, Qi Ming, Wentao Wang, Qi Tian, and Junchi Yan. Learning high-precision bounding box for rotated object detection via kullback-leibler divergence. In *Advances in Neural Information Processing Systems*, volume 34, pages 18381–18394, 2021.
- [38] Xue Yang, Gefan Zhang, Xiaojiang Yang, Yue Zhou, Wentao Wang, Jin Tang, Tao He, and Junchi Yan. Detecting rotated objects as gaussian distributions and its 3-d generalization. *IEEE Transactions on Pattern Analysis and Machine Intelligence*, 2022.
- [39] Xue Yang, Yue Zhou, Gefan Zhang, Jirui Yang, Wentao Wang, Junchi Yan, Xiaopeng Zhang, and Qi Tian. The kfou loss for rotated object detection. In *International Conference on Learning Representations*, 2023.
- [40] Ze Yang, Shaohui Liu, Han Hu, Liwei Wang, and Stephen Lin. Reppoints: Point set representation for object detection. In *IEEE/CVF International Conference on Computer Vision*, pages 9656–9665, 2019.
- [41] Liping Hou, Ke Lu, Xue Yang, Yuqiu Li, and Jian Xue. G-rep: Gaussian representation for arbitrary-oriented object detection. *arXiv preprint arXiv:2205.11796*, 2022.
- [42] Wentong Li, Yijie Chen, Kaixuan Hu, and Jianke Zhu. Oriented reppoints for aerial object detection. In *IEEE/CVF Conference on Computer Vision and Pattern Recognition*, pages 1829–1838, 2022.
- [43] Anna Khoreva, Rodrigo Benenson, Jan Hosang, Matthias Hein, and Bernt Schiele. Simple does it: Weakly supervised instance and semantic segmentation. In *IEEE Conference on Computer Vision and Pattern Recognition*, pages 876–885, 2017.
- [44] Cheng-Chun Hsu, Kuang-Jui Hsu, Chung-Chi Tsai, Yen-Yu Lin, and Yung-Yu Chuang. Weakly supervised instance segmentation using the bounding box tightness prior. *Advances in Neural Information Processing Systems*, 32, 2019.

- [45] Kaiming He, Georgia Gkioxari, Piotr Dollár, and Ross Girshick. Mask r-cnn. In *IEEE International Conference on Computer Vision*, pages 2961–2969, 2017.
- [46] Zhi Tian, Chunhua Shen, and Hao Chen. Conditional convolutions for instance segmentation. In *European Conference on Computer Vision*, pages 282–298, 2020.
- [47] Javed Iqbal, Muhammad Akhtar Munir, Arif Mahmood, Afsheen Razaqat Ali, and Mohsen Ali. Leveraging orientation for weakly supervised object detection with application to firearm localization. *Neurocomputing*, 440:310–320, 2021.
- [48] Tianyu Zhu, Bryce Ferenczi, Pulak Purkait, Tom Drummond, Hamid Rezaatofghi, and Anton van den Hengel. Knowledge combination to learn rotated detection without rotated annotation. In *IEEE/CVF Conference on Computer Vision and Pattern Recognition*, 2023.
- [49] Zhiwen Tan, Zhiguo Jiang, Chen Guo, and Haopeng Zhang. Wsodet: A weakly supervised oriented detector for aerial object detection. *IEEE Transactions on Geoscience and Remote Sensing*, 61:1–12, 2023.
- [50] Kaiming He, Xiangyu Zhang, Shaoqing Ren, and Jian Sun. Deep residual learning for image recognition. In *IEEE Conference on Computer Vision and Pattern Recognition*, pages 770–778, 2016.
- [51] Tsung-Yi Lin, Piotr Dollár, Ross Girshick, Kaiming He, Bharath Hariharan, and Serge Belongie. Feature pyramid networks for object detection. In *IEEE Conference on Computer Vision and Pattern Recognition*, pages 936–944, 2017.
- [52] Jiahui Yu, Yuning Jiang, Zhangyang Wang, Zhimin Cao, and Thomas Huang. Unitbox: An advanced object detection network. In *Proceedings of the 24th ACM International Conference on Multimedia*, pages 516–520, 2016.
- [53] Adam Paszke, Sam Gross, Francisco Massa, Adam Lerer, James Bradbury, Gregory Chanan, Trevor Killeen, Zeming Lin, Natalia Gimelshein, Luca Antiga, Alban Desmaison, Andreas Kopf, Edward Yang, Zachary DeVito, Martin Raison, Alykhan Tejani, Sasank Chilamkurthy, Benoit Steiner, Lu Fang, Junjie Bai, and Soumith Chintala. Pytorch: An imperative style, high-performance deep learning library. In *Advances in Neural Information Processing Systems*, volume 32, pages 8024–8035, 2019.
- [54] Yue Zhou, Xue Yang, Gefan Zhang, Jiabao Wang, Yanyi Liu, Liping Hou, Xue Jiang, Xingzhao Liu, Junchi Yan, Chengqi Lyu, Wenwei Zhang, and Kai Chen. Mmrotate: A rotated object detection benchmark using pytorch. In *Proceedings of the 30th ACM International Conference on Multimedia*, 2022.
- [55] Shi-Min Hu, Dun Liang, Guo-Ye Yang, Guo-Wei Yang, and Wen-Yang Zhou. Jittor: a novel deep learning framework with meta-operators and unified graph execution. *Science China Information Sciences*, 63:1–21, 2020.
- [56] Liping Hou, Ke Lu, Jian Xue, and Yuqiu Li. Shape-adaptive selection and measurement for oriented object detection. In *Proceedings of the AAAI Conference on Artificial Intelligence*, volume 36, pages 923–932, 2022.
- [57] Zonghao Guo, Chang Liu, Xiaosong Zhang, Jianbin Jiao, Xiangyang Ji, and Qixiang Ye. Beyond bounding-box: Convex-hull feature adaptation for oriented and densely packed object detection. In *IEEE/CVF Conference on Computer Vision and Pattern Recognition*, pages 8788–8797, 2021.
- [58] Ze Liu, Yutong Lin, Yue Cao, Han Hu, Yixuan Wei, Zheng Zhang, Stephen Lin, and Baining Guo. Swin transformer: Hierarchical vision transformer using shifted windows. In *IEEE/CVF International Conference on Computer Vision*, pages 9992–10002, 2021.
- [59] Xian Sun, Peijin Wang, Zhiyuan Yan, Feng Xu, Ruiping Wang, Wenhui Diao, Jin Chen, Jihao Li, Yingchao Feng, Tao Xu, Martin Weinmann, Stefan Hinz, Cheng Wang, and Kun Fu. Fair1m: A benchmark dataset for fine-grained object recognition in high-resolution remote sensing imagery. *ISPRS Journal of Photogrammetry and Remote Sensing*, 184:116–130, 2022.
- [60] Ilya Loshchilov and Frank Hutter. Decoupled weight decay regularization. In *International Conference on Learning Representations*, 2018.
- [61] Alexey Dosovitskiy, Lucas Beyer, Alexander Kolesnikov, Dirk Weissenborn, Xiaohua Zhai, Thomas Unterthiner, Mostafa Dehghani, Matthias Minderer, Georg Heigold, Sylvain Gelly, et al. An image is worth 16x16 words: Transformers for image recognition at scale. In *International Conference on Learning Representations*, 2021.